DALTON

# Towards synthetic models for trinuclear copper active sites of ascorbate oxidase and laccase: self-assembly, crystal structure and magnetic properties of the copper(II) complexes of 1,3,5-tris(1,4,7-triazacyclonon-1-ylmethyl)benzene †

**Leone Spiccia,*[a] Bim Graham,[a] Milton T. W. Hearn,[b] George Lazarev,[a] Boujemaa Moubaraki,[a] Keith S. Murray *[a] and Edward R. T. Tiekink[c]**

[a] *Department of Chemistry, Monash University, Clayton, Victoria 3168, Australia*
[b] *Centre for Bioprocess Technology and Department of Biochemistry, Monash University, Clayton, Victoria 3168, Australia*
[c] *Department of Chemistry, University of Adelaide, 5005, Australia*

Reaction of the hydrobromide salt of 1,3,5-tris(1,4,7-triazacyclonon-1-ylmethyl)benzene, L·9HBr, with copper(II) nitrate followed by cation-exchange chromatographic purification afforded $[Cu_3L(H_2O)_6][ClO_4]_6\cdot 6H_2O$ **1**. The ESR and magnetic susceptibility data indicated that the complex consists of three identical non-interacting copper(II) centres. Reaction of **1** with a phosphate source produces $\{[Cu_3L(\mu\text{-}OH)(\mu_3\text{-}HPO_4)(H_2O)][PF_6]_3\cdot 3H_2O\}_n$ **2** the polymeric lattice of which contains trinuclear copper(II) sites with structural similarities to laccase (Lc) and ascorbate oxidase (AO). These trinuclear sites consist of two type 3 copper(II) centres, at a separation of 3.557(4) Å, linked by an hydroxo bridge and two phosphate oxygens while another phosphate oxygen links these two centres to the further removed type 2 copper(II) centre, establishing separations of 4.561(4) and 5.474(4) Å. The magnetic properties of **2** were investigated in the temperature range 4.2–300 K and they revealed an $S = \frac{1}{2}$ molecular ground state arising from antiferromagnetic coupling. A number of models have been employed in order quantitatively to fit the $\mu_{eff}$ *versus* temperature data including those applicable to the resting oxidised state of laccase and ascorbate oxidase, *vis-à-vis* dimer plus uncoupled monomer, but the best fits were obtained using a symmetrical trinuclear approximation with $J_{12}$ for the doubly bridged $[CuL(\mu\text{-}OH)(\mu\text{-}HPO_4)Cu]$ moiety of $-53$ or *ca.* $-80$ cm$^{-1}$ combined respectively with $J$ for the two equal three-atom phosphato bridges of $-90$ or $-77$ to $-90$ cm$^{-1}$. The 77 K solid-state ESR spectrum of **2** is unusual for $S = \frac{1}{2}$ ground-state systems and shows six components of a probable seven-line copper hyperfine multiplet between 2500 and 3100 G and a strong $x$, $y$ resonance at *ca.* 3200 G, most probably due to weak copper(II) pair interactions or the superimposition of $S = \frac{1}{2}$ signals from both molecular doublets. The 77 K solution ESR spectrum (dimethylformamide, water–glycol 1 : 1) for **2** is typical of a monomeric copper(II) centre and closely resembles the ESR spectrum of the type 2 site in Lc and AO. The ESR, electrospray mass spectrometric and NMR data indicate that **2** dissociates in solution to give a trinuclear unit consisting of two type 3 copper(II) centres (ESR silent), which are linked by the hydroxo and phosphate group (phosphate is released from the complex only on addition of acid), and an isolated type 2 copper(II) centre which is probably responsible for the ESR features.

The presence of multinuclear arrays of copper centres at the active sites of copper oxidases and oxygen-transport proteins continues to stimulate interest in model compounds which closely mimic the structure, properties and function of these biosites.[1] In recent years, much attention has been directed at binuclear copper complexes which mimic the function of hemocyanin, an oxygen carrier in molluscs and arthropods, and tyrosinase, an enzyme catalysing the hydroxlyation of phenols to *o*-diphenols and the conversion of the latter into *o*-diquinones. Through the use of low-molecular-weight compounds, important aspects of the mechanism of oxygen transport and activation have been elucidated.[1–7] These and other copper compounds also model either the mononuclear (type 1 and type 2) or the binuclear type 3 copper centres found in ascorbate oxidase (AO) and laccase (Lc). In contrast, compounds which model the structure and physical properties of the entire trinuclear metal site in these enzymes, consisting of one type 2 and two type 3 copper centres,[8–10] are relatively scarce but have attracted recent attention. A number of studies have reported symmetric and asymmetric trinuclear copper complexes[11–16] as structural models for these biosites and there is a very recent report of a trinuclear, mixed-valence complex, *vis-à-vis* $Cu^{II}_2Cu^{III}$, isolated following oxidation of the trigonal-planar copper(I) complex of *N*-permethylated cyclohexane-1,2-diamine.[17] This has raised questions about the involvement of copper(III) in the function of the enzymes.

Our initial studies aimed at model compounds for trinuclear biosites in general, but more specifically AO and Lc, have led to the development of the potentially trinucleating ligand 1,3,5-tris(1,4,7-triazacyclonon-1-ylmethyl)benzene, L, which is capable of binding three metal centres in close proximity. This ligand has been applied in the synthesis of $[Cu_3L(H_2O)_6][ClO_4]_6\cdot 6H_2O$ **1**. When **1** is left in aqueous solution, in the presence of $PF_6^-$ ions, slow hydrolysis of $PF_6^-$ occurs, leading to the self-assembly of $\{[Cu_3L(\mu\text{-}OH)(\mu_3\text{-}HPO_4)(H_2O)][PF_6]_3\cdot 3H_2O\}_n$ **2**. Complex **2** contains trinuclear metal sites in which three copper(II) centres are linked by an $HPO_4^{2-}$ phosphate bridge and two of the coppers are further linked by an hydroxo bridge (Fig. 1) and is a good model for the zinc enzymes, phospholipase C, phosphate-modified phospholipase C and P1

† Based on the presentation given at Dalton Discussion No. 2, 2nd–5th September 1997, University of East Anglia, UK.

*Non-SI units employed:* $\mu_B \approx 9.27 \times 10^{-24}$ J T$^{-1}$, G = $10^{-4}$ T.

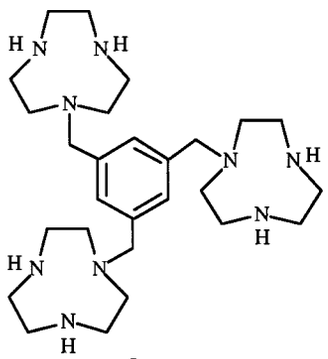

L

nuclease.[18] The complex can also be viewed as two type 3 coppers ($\mu$-$HPO_4^{2-}$, $\mu$-OH) connected to a more remotely displaced type 2 copper by $HPO_4^{2-}$ and therefore has relevance to the active sites of AO and Lc. We report here the structure of **2** as well as magnetic and ESR studies on **1** and **2** and a comparison of these properties to those of AO and Lc.

## Experimental

### Materials and reagents

Reagent or analytical grade materials were obtained from commercial suppliers and used without further purification. 1,4,7-Triazatricyclo[5.2.1.0$^{4,10}$]decane was prepared from 1,4,7-triazacyclononane as described by Zompa and co-workers.[19] 1,3,5-Tri(bromomethyl)benzene was synthesized according to a published method.[20]

### Physical measurements

Proton and $^{13}C$ NMR spectra for $D_2O$ solutions of L were recorded on a Bruker AC200 spectrometer and referenced relative to an internal standard of $Na(O_2CCD_2CD_2SiMe_3)$ and an external standard of tetramethylsilane, respectively. Phosphorus-31 NMR spectra for dimethylformamide (dmf) solutions of **2** on a Bruker AM300 spectrometer and referenced relative to an external standard of 85% $H_3PO_4$. Infrared spectra on a Perkin-Elmer 1600 FTIR spectrophotometer as KBr pellets and electronic spectra on a Cary 5 spectrophotometer. Electrospray mass spectra were recorded in water on a Micromass Platform quadrupole mass spectrometer using a cone voltage of 25 V. Electron microprobe analyses were made with a JEOL JSM-1 scanning electron microscope through an NEC X-ray detector and pulse-processing system connected to a Packard multichannel analyser. Microanalyses were performed by Chemical and Micro Analytical Services (CMAS), Melbourne, Australia. The ESR spectra were recorded at 77 K on a Varian E-12 spectrometer operating at *ca.* 9.6 GHz (X-band). Samples were run as powders or dilute solutions in normal 3 mm inside diameter tubes and frozen in a liquid-nitrogen-flow cryostat. Variable-temperature magnetic susceptibility measurements were made using a Quantum Design MPMS SQUID magnetometer operating in an applied field of 1 T. The powdered samples were contained in calibrated gelatine capsules which were held in the centre of a straw, the latter being attached to the end of the sample rod. The temperature and field were checked against a standard palladium sample and $CuSO_4 \cdot 5H_2O$. Fitting of the magnetic data employed a non-linear least-squares program POLYMER which was written at Monash University.

**CAUTION:** although no problems were encountered in this work, transition-metal perchlorates are potentially explosive and should thus be prepared in small quantities and handled with care.

### Preparations

**1,3,5-Tris(1,4,7-triazacyclonon-1-ylmethyl)benzene nonahydrobromide L·9HBr.** A solution of 1,3,5-tri(bromomethyl)-benzene (1.62 g, 4.5 mmol) in dry acetonitrile (50 cm$^3$) was added dropwise to a stirred solution of 1,4,7-triazatricyclo-[5.2.1.0$^{4,10}$]decane (2.00 g, 14.4 mmol) in dry acetonitrile (50 cm$^3$) over 2 h, resulting in the formation of a white precipitate. After stirring overnight, the precipitate was filtered off, washed with acetonitrile (10 cm$^3$) and dried in a vacuum desiccator. The solid was then dissolved in distilled water (20 cm$^3$) and refluxed for 4 h. Sodium hydroxide pellets (4.00 g, 100 mmol) were carefully added in portions to the solution and refluxing continued for 4 h. Toluene (100 cm$^3$) was then added to the solution and the water distilled off using a Dean–Stark azeotropic apparatus. The toluene solution was filtered while hot to remove the precipitate of NaBr and NaOH which formed. The solid residue was then extracted twice with hot toluene (200 cm$^3$) and the combined toluene fractions evaporated to dryness on a Rotavap to yield a light yellow oil. This was dissolved in distilled water (5 cm$^3$) and concentrated HBr (50 cm$^3$) and absolute ethanol (50 cm$^3$) added dropwise to afford a white precipitate. Recrystallisation of the precipitate from a mixture of water and concentrated HBr yielded the pure product as a white microcrystalline solid (4.20 g, 76%) (Found: C, 26.4; H, 5.0; N, 10.0. $C_{27}H_{60}Br_9N_9$ requires C, 26.4; H, 4.9; N, 10.3%). $\delta_H$(200.13 MHz) 3.09 (12 H, t, tacn ring $CH_2$), 3.33 (12 H, t, tacn ring $CH_2$), 3.69 (12 H, s, tacn ring $CH_2$), 4.02 (6 H, s, $NCH_2C_6H_3$) and 7.54 (3 H, s, aromatic CH); $\delta_C$(50.32 MHz) 41.94, 43.46, 47.07 (tacn ring $CH_2$), 57.90 $NCH_2C_6H_3$), 131.81 (aromatic CH) and 135.83 (aromatic quaternary C).

**$[Cu_3L(H_2O)_6][ClO_4]_6 \cdot 6H_2O$ 1.** To a solution of L·9HBr (1.00 g, 0.81 mmol) and $Cu(NO_3)_2 \cdot 3H_2O$ (0.61 g, 2.52 mmol) dissolved in distilled water (50 cm$^3$) was added NaOH solution (2 mol dm$^{-3}$) until a precipitate of copper hydroxide began to appear. Sufficient dilute HCl (2 mol dm$^{-3}$) was then added just to dissolve the precipitate. The resulting dark blue solution was diluted to 2 dm$^3$ with distilled water and loaded onto a Sephadex SP-C25 cation-exchange column ($H^+$ form, 15 × 4 cm). After washing the column with distilled water and 0.2 mol dm$^{-3}$ sodium perchlorate solution to remove a light green band of excess of $Cu^{2+}$, a dark blue band was eluted with 1.0 mol dm$^{-3}$ sodium perchlorate solution. This fraction was concentrated to about 50 cm$^3$ on a Rotavap and then left slowly to evaporate. Blue crystals of the product formed, which were filtered off and air-dried (0.42 g, 34%). Samples for analysis were washed quickly with a small amount of cold methanol (Found: C, 21.5; H, 4.5; N, 8.2. Calc. for $C_{27}H_{75}Cl_6Cu_3N_9O_{36}$: C, 21.5; H, 5.0; N, 8.4%); $\tilde{\nu}_{max}$/cm$^{-1}$ 3454s (br), 3300m, 2935w, 1628s (br), 1490m, 1456s, 1358m, 1083s (br), 827 m and 628s; $\lambda_{max}$/nm ($\varepsilon$/dm$^3$ mol$^{-1}$ cm$^{-1}$): (water) 640 (vbr) (150); (dmf) 640 (vbr) (200). Electron microprobe: Cu, Cl uniformly present.

**$\{[Cu_3L(\mu\text{-}OH)(\mu_3\text{-}HPO_4)(H_2O)][PF_6]_3 \cdot 3H_2O\}_n$, 2.** *Method A.* Compound **1** (0.100 g, 0.066 mmol) was dissolved in water (5 cm$^3$) and adjusted to pH 7–7.5 with NaOH solution (1 mol dm$^{-3}$). The salt $KPF_6$ (1 g) was then added, giving a blue precipitate. This was dissolved by adding water (20 cm$^3$) and heating on a steam-bath. The filtered solution was left to evaporate, yielding dark blue crystals suitable for X-ray crystallography after 2 weeks. These were filtered off, washed with methanol and air dried (0.025 g, 29%).

*Method B.* Compound **1** (0.044 g, 0.029 mmol) and $Na_2HPO_4 \cdot 12H_2O$ (0.011 g, 0.031 mmol) were dissolved in distilled water (10 cm$^3$) and a saturated solution (3 cm$^3$) of $KPF_6$ added. This produced an immediate blue precipitate. After cooling in a refrigerator for 1 h the product was filtered off, washed with methanol and air dried (0.027 g, 70%) (Found: C, 24.6; H, 4.6; N, 9.4. Calc. for $C_{27}H_{61}Cu_3F_{18}N_9O_9P_4$: C, 24.7; H, 4.7; N, 9.6%);

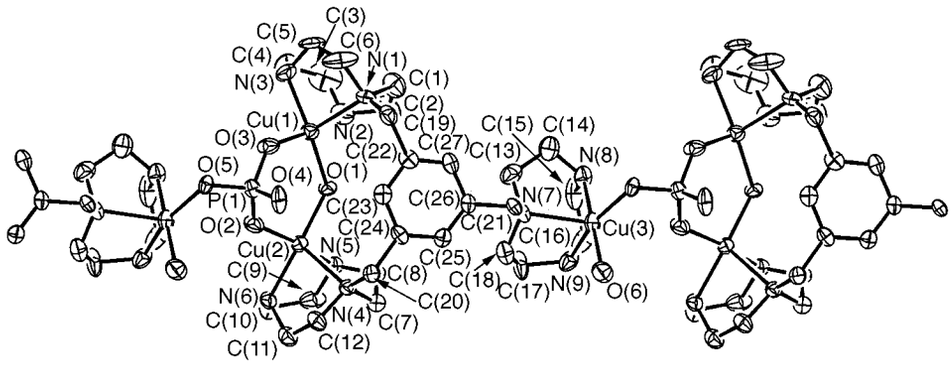


**Fig. 1** Molecular structure of the repeating cation unit in the polymer $\{[Cu_3L(\mu\text{-}OH)(\mu_3\text{-}HPO_4)(H_2O)][PF_6]_3\cdot 3H_2O\}_n$ showing the crystallographic numbering scheme employed

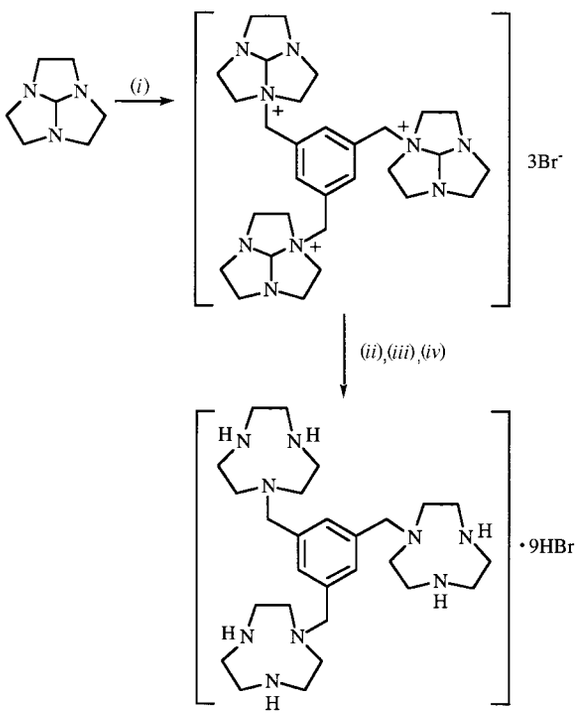


**Scheme 1** Preparation of the nonahydrobromide salt of L: (*i*) 1,3,5-tri(bromomethyl)benzene, MeCN, 2 h; (*ii*) water, reflux, 4 h; (*iii*) NaOH, reflux, 4 h; (*iv*) aqueous HBr

$\tilde{\nu}/cm^{-1}$ (KBr) 3450s (br), 3344m, 2948w, 1638w, 1493w, 1460m, 1100s, 843s and 559s; $\lambda_{max}/nm$ ($\varepsilon/dm^3\ mol^{-1}\ cm^{-1}$): (water) 646 (vbr) (195); (dmf) 645 (229). Electron microprobe: Cu, P, F uniformly present, Cl absent.

### Crystallography

A dark blue needle (0.40 × 0.13 × 0.10 mm) of compound **2** was used for single-crystal X-ray diffraction data collection. Crystal data and details of data collection are given in Table 1. Diffraction data were collected at 293 K on a Rigaku AFC6R diffractometer (Mo-Kα radiation). Cell constants were obtained from a least-squares refinement using the setting angles of 25 carefully centred reflections in the range $31.0 < 2\theta < 32.6°$. The ω–2θ scan technique, $3 < \theta < 27.5°$, was used to measure 11 905 data (11 432 unique) from which 3764 reflections with $I \geqslant 3.0\sigma(I)$ were used in the refinement. Corrections were applied for absorption effects (DIFABS)[21] and for crystal decay during the data collection. The structure was solved with DIRDIF 92[22] and refined with TEXSAN.[23] Non-hydrogen atoms were refined with anisotropic thermal parameters and H atoms were included in idealised geometric positions (C–H 0.97, N–H 0.95 Å) and were not refined. Refinement against *F* [sigma weights, *i.e.* $1/\sigma^2(F)$] converged with agreement factors of

**Table 1** Crystallographic data for $\{[Cu_3L(\mu\text{-}OH)(\mu_3\text{-}HPO_4)(H_2O)][PF_6]_3\cdot 3H_2O\}_n$ **2**

| | |
|---|---|
| Formula | $C_{27}H_{61}Cu_3F_{18}N_9O_9P_4$ |
| *M* | 1312.34 |
| Crystal system | Triclinic |
| Space group | $P\bar{1}$ (no. 2) |
| *a*/Å | 15.010(8) |
| *b*/Å | 15.894(8) |
| *c*/Å | 13.629(6) |
| α/° | 101.85(4) |
| β/° | 114.23(4) |
| γ/° | 64.88(5) |
| *U*/Å$^3$ | 2682(2) |
| *Z* | 2 |
| *T*/K | 293(1) |
| λ/Å | 0.7107 (Mo-Kα) |
| $D_c$/g cm$^{-3}$ | 1.624 |
| *F*(000) | 1334 |
| μ(Mo-Kα)/cm$^{-1}$ | 14.11 |
| Transmission factor range | 0.961–1.000 |
| $2\theta_{max}$/°; *hkl* data collected | 55; $+h, \pm k, \pm l$ |
| No. data measured | 11 905 |
| No. unique data | 11 432 |
| No. observed data [$I \geqslant 3\sigma(I)$] | 3764 |
| No. parameters refined | 540 |
| $R^a$ | 0.093 |
| $R'^b$ | 0.107 |
| Goodness of fit[c] | 3.33 |
| Maximum Δ/σ | 0.067 |
| Maximum Δρ/e Å$^{-3}$ | 1.10 |

[a] $R(F) = \Sigma(|F_o| - |F_c|)/\Sigma|F_o|$. [b] $R' = [\Sigma w(|F_o| - |F_c|)^2/\Sigma w|F_o|^2]^{\frac{1}{2}}$, $w = [\sigma^2\cdot(F_o)]^{-1}$. [c] $[\Sigma w(|F_o| - |F_c|)^2/(N_{obs} - N_{param})]^{\frac{1}{2}}$.

$R = 0.093$, $R' = 0.107$ for 3764 reflections and 540 parameters. Scattering factors for all atoms were those incorporated in the TEXSAN program. The atomic numbering scheme for the cation is shown in Fig. 1, which was drawn with the ORTEP program.[24] Selected interatomic distances and bond angles are given in Table 2.

CCDC reference number 186/673.

## Results and Discussion

### Synthesis and crystal structure

The tris(1,4,7-triazacyclonon-1-yl) ligand, L, was prepared following the method described in Scheme 1. Reaction of 3 equivalents of 1,4,7-triazatricyclo[5.2.1.0$^{4,10}$]decane, the tricyclic orthoamide derivative of 1,4,7-triazacyclononane, with 1,3,5-tri(bromomethyl)benzene affords the tris(amidinium) salt, which following base hydrolytic work-up gives an aqueous solution of the target macrocycle. Addition of hydrobromic acid precipitates the nonahydrobromide salt the composition of which was established by elemental analyses and $^1$H and $^{13}$C NMR spectroscopy.

**Table 2** Selected intramolecular distances (Å) and bond angles (°) for compound **2**

| | | | | | |
|---|---|---|---|---|---|
| Cu(1)–O(1) | 1.89(1) | Cu(1)–O(3) | 1.94(1) | Cu(1)–N(1) | 2.33(2) |
| Cu(1)–N(2) | 2.01(2) | Cu(1)–N(3) | 2.02(2) | Cu(2)–O(1) | 1.96(2) |
| Cu(2)–O(2) | 1.94(1) | Cu(2)–N(4) | 2.36(1) | Cu(2)–N(5) | 2.02(1) |
| Cu(2)–N(6) | 2.03(2) | Cu(3)–O(5) | 1.97(1) | Cu(3)–O(6) | 2.00(1) |
| Cu(3)–N(7) | 2.29(2) | Cu(3)–N(8) | 1.96(2) | Cu(3)–N(9) | 2.01(2) |
| P(1)–O(2) | 1.50(1) | P(1)–O(3) | 1.52(2) | P(1)–O(4) | 1.59(1) |
| P(1)–O(5) | 1.54(1) | Cu(1)···Cu(2) | 3.557(4) | Cu(1)···Cu(3′) | 5.474(4) |
| Cu(2)···Cu(3′) | 4.561(4) | | | | |

| | | | | | | | |
|---|---|---|---|---|---|---|---|
| O(1)–Cu(1)–O(3) | 95.2(6) | O(1)–Cu(1)–N(1) | 106.4(6) | O(2)–Cu(2)–N(6) | 89.8(7) | N(4)–Cu(2)–N(5) | 81.5(5) |
| O(1)–Cu(1)–N(2) | 88.8(7) | O(1)–Cu(1)–N(3) | 167.2(6) | N(4)–Cu(2)–N(6) | 83.0(7) | N(5)–Cu(2)–N(6) | 82.5(7) |
| O(3)–Cu(1)–N(1) | 107.7(6) | O(3)–Cu(1)–N(2) | 168.6(7) | O(5)–Cu(3)–O(6) | 90.5(6) | O(5)–Cu(3)–N(7) | 114.5(5) |
| O(3)–Cu(1)–N(3) | 90.4(7) | N(1)–Cu(1)–N(2) | 81.2(8) | O(5)–Cu(3)–N(8) | 91.8(7) | O(5)–Cu(3)–N(9) | 161.3(6) |
| N(1)–Cu(1)–N(3) | 82.7(9) | N(2)–Cu(1)–N(3) | 83.7(8) | O(6)–Cu(3)–N(7) | 97.4(6) | O(6)–Cu(3)–N(9) | 92.6(7) |
| O(1)–Cu(2)–O(2) | 93.6(6) | O(1)–Cu(2)–N(4) | 103.9(6) | N(7)–Cu(3)–N(8) | 83.8(7) | N(7)–Cu(3)–N(9) | 83.3(6) |
| O(1)–Cu(2)–N(5) | 91.9(7) | O(1)–Cu(2)–N(6) | 170.5(5) | N(8)–Cu(3)–N(9) | 84.4(8) | | |
| O(2)–Cu(2)–N(4) | 111.7(5) | O(2)–Cu(2)–N(5) | 163.9(6) | | | | |

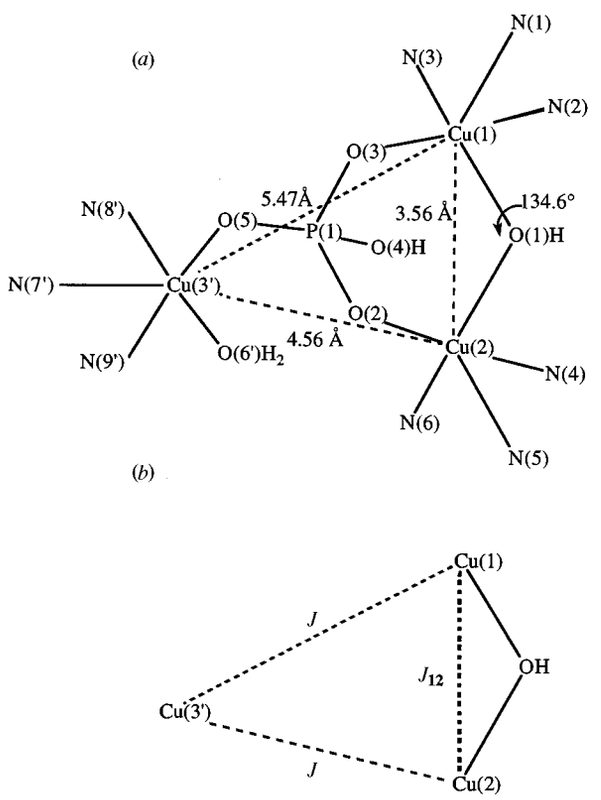


**Fig. 2** Schematic diagram of the repeat trinuclear framework of complex **2** showing (*a*) the Cu···Cu separations and Cu–O(H)–Cu angle and (*b*) the designated *J* values for an isosceles triangle approximation

The complex $[Cu_3L(H_2O)_6][ClO_4]_6\cdot 6H_2O$ **1** was prepared by treating L·9HBr with $Cu(NO_3)_2\cdot 3H_2O$ followed by pH adjustment and cation-exchange chromatography purification with $NaClO_4$ solution as the eluent. Blue crystals of $\{[Cu_3L(\mu\text{-}OH)(\mu_3\text{-}HPO_4)(H_2O)][PF_6]_3\cdot 3H_2O\}_n$ **2** were initially formed when an aqueous solution of **1** containing an excess of $KPF_6$ was allowed to stand at pH ≈ 7.5 for 1 week. Phosphate is generated by the hydrolysis of $PF_6^-$. Although usually slow,[25] this conversion does occur in solutions of the zinc(II) complex of 1-(2-hydroxyethyl)-1,4,7,10-tetraazacyclododecane.[25c] The complex is obtained in greater yield (70%) by direct reaction of **1** with a phosphate source ($Na_2HPO_4$) in the presence of $KPF_6$. The $^{31}P$ NMR spectrum of **1** in dmf shows only a septet due to $PF_6^-$ (δ −139.7, $J_{PF}$ = 709 Hz), suggesting that the phosphate is co-ordinated to the paramagnetic copper(II) centres. Following acidification a singlet is observed at δ 5.0 (1 : 3 ratio relative to $PF_6^-$ signal), confirming the presence of phosphate.

The crystal structure of compound **2** comprises $[LCu_2(\mu\text{-}OH)(\mu_3\text{-}HPO_4)Cu(OH_2)]^{3+}$ cations, $PF_6^-$ anions and water of crystallisation in the ratio 1 : 3 : 3. The cation, illustrated in Fig. 1, features three copper(II) centres each co-ordinated to the three nitrogen atoms of separate triazamacrocycles of L. The $HPO_4^{2-}$ dianion further links the three centres generating a linear polymeric structure throughout the lattice which is propagated in the crystallographic *c* direction; connections between the linear chains are afforded by intermolecular hydrogen-bonding contacts. An hydroxo bridge links Cu(1) and Cu(2), and a water molecule completes the Cu(3) co-ordination sphere. The cation therefore carries a 3+ charge which is balanced by three $PF_6^-$ ions. Although the NH and OH hydrogen atoms could not be located in the refinement, strong support for the proposed assignment is found in the molecular conformations of the triazamacrocycles, the length of the P–O(4) bond compared to the other P–O distances, the nature of the hydrogen-bonding interactions and the $^{31}P$ NMR spectrum. Specifically, there are O–H···F and O–H···O contacts involving the bridging $OH^-$ and $HPO_4^{2-}$ anions. A close O–H···F(5) contact [O···F 3.13(2) Å] is noted involving bridging $OH^-$ which causes F(5) to approach Cu(1) [3.45(2) Å] and more significantly Cu(2) [Cu···F 3.18(2) Å]. Similarly, a PO–H···O(1w) (O···O 2.70 Å) contact is found. The O(1w) water molecule forms three additional contacts, one further acceptor contact [O···O(6) is 2.81(2) Å] and two donor contacts, *i.e.* O···O(5) is 2.66(2) Å and O···F(13) is 2.81(3) Å, confirming the assignment of the PO–H···O(1w) interaction.

Each copper(II) centre exists in a tetragonally distorted square-pyramidal geometry with each basal plane being defined by an $N_2O_2$ donor set and a tertiary N atom in the apical position. The arrangement of each tacn macrocycle and relevant bond distances and angles (Table 2) correspond to those found in square-pyramidal copper(II) complexes of tacn and bis(tacn) macrocycles.[19,26]

The crystal structure has confirmed that although compound **2** is polymeric, it does contain trinuclear copper sites (Figs. 1 and 2) with structural similarities to AO and Lc, which exhibit $Cu_3$ sites consisting of two linked type 3 coppers and one type 2 copper as well as a more remote type 1 copper.[8–10] The trinuclear sites in **2** contain three copper(II) centres in a distorted square-pyramidal geometry. The site can be considered as two ESR-silent (see below) type 3 copper centres separated by 3.557(4) Å and linked by an hydroxo bridge and two phosphate oxygens. The existence of two Cu–OH distances of 1.89(1) and 1.96(2) Å in **2** highlights the asymmetric nature of the Cu(1)–OH–Cu(2) bridging unit. In **2** another oxygen from the phosphate group further links these two copper centres to the third

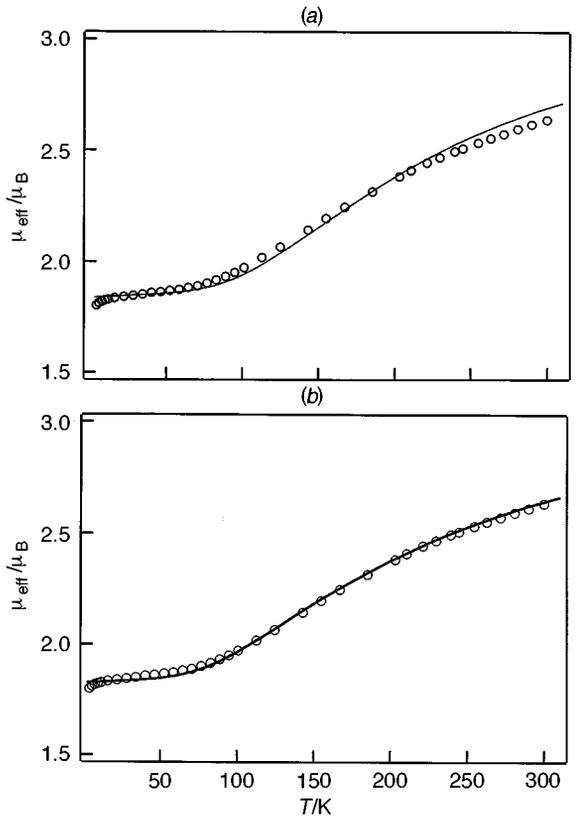


**Fig. 3** Plot of $\mu_{eff}$ (per $Cu_3$) *versus* temperature for complex **2**. The solid line was calculated using: (*a*) a monomer + dimer model with the best fit by equation (1) yielding $g_1 = 2.10$, $g_2 = 2.12$, $J_{12} = -161$ $cm^{-1}$ and $N_\alpha = 180 \times 10^{-6}$ $cm^3$ $mol^{-1}$; (*b*) a non-symmetrical trinuclear model with the best fit by equation (6) yielding $g = 2.10$, $\Delta_1 = 92$ $cm^{-1}$, $\Delta_2 = 274$ $cm^{-1}$ and $N_\alpha = 180 \times 10^{-6}$ $cm^3$ $mol^{-1}$

type 2 copper centre, establishing longer Cu · · · Cu separations of 4.561(4) and 5.474(4) Å. Across the aromatic mesitylene spacer, the Cu(1) · · · Cu(3) and Cu(2) · · · Cu(3) distances are 9.426(4) and 9.279(4) Å. Fenton and co-workers[15] have reported the trinuclear copper(II) complex of a trinucleating Schiff-base ligand in which the separation between the type 3 coppers of 3.62 Å is similar to those in compound **2**. The distances to the type 2 copper are slightly longer, *vis-à-vis* 4.95 and 5.89 Å, due to the absence of a bridging group. For both complexes, however, the M · · · M separations are longer than in the trinuclear site of AO (3.66, 3.78 and 3.68 Å), and the copper co-ordination numbers are higher than in the enzyme.[8b] The co-ordination number, geometry and description of the ligand field around each copper in the enzyme is still a subject for debate.[10] There have been suggestions that the ligand field about the type 2 copper is square planar with a free equatorial site oriented towards the type 3 coppers while that around the type 3 coppers is best described as trigonal bipyramidal with a free equatorial site for substrate attachment. The various Cu · · · Cu distances in **2** better match the distances in azide- and peroxo-modified AO, although the hydroxo group linking the two type 3 coppers is no longer present in the modified enzyme. For the modified enzymes[8b] the type 3–type 3 copper separations are 5.1 (4.8) Å and the type 2–type 3 copper separations 3.6 (4.5) and 4.6 (3.7) Å (distances for peroxo-modified AO in parentheses). Although **2** does not fully replicate the structural features of the enzyme, the self-assembly of the trinuclear site in **2** indicates that, with judicious choice of the components, trinuclear sites can be assembled in solution and this feature exploited in reactivity studies.

### Magnetic susceptibility and ESR measurements

Magnetic susceptibilities were determined for complexes **1** and **2** over the temperature range 4.2–300 K in an applied field of 1 T. The data for **1** are compatible with an 'isolated' trinuclear structure in which the three $Cu^{II}$(tacn) moieties do not interact magnetically across the central aromatic mesitylene spacer unit. Thus a plot of $\chi_m^{-1}$ *versus* temperature (per $Cu_3$) essentially follows a Curie temperature dependence $\chi_m = C/T$ with a $C$ value of 1.25 $cm^3$ $mol^{-1}$ $K^{-1}$. The corresponding $\mu_{eff}$ values are 3.23 $\mu_B$ (1.86 $\mu_B$ per Cu) over the whole temperature range except for a very small decrease below 10 K. The X-band ESR spectrum of **1** in frozen dmf solution shows a typical mononuclear near-axial copper(II) signal which was simulated with the aid of the Bruker SIMFONIA program using parameters $g_z = 2.28$, $A_z = 169 \times 10^{-4}$ $cm^{-1}$, $g_x = 2.06$, $A_x = 0 \times 10^{-4}$ $cm^{-1}$, $g_y = 2.06$ and $A_y = 24 \times 10^{-4}$ $cm^{-1}$.

The magnetic moment, per $Cu_3$, for complex **2** decreases from 2.63 $\mu_B$ to a plateau of 1.86 $\mu_B$ between 60 and 10 K with a small decrease occurring between 10 and 4.2 K (Fig. 3). This behaviour is indicative of medium-strength antiferromagnetic coupling, leading to a spin doublet, $S = \frac{1}{2}$ ground state. The trinuclear unit in the structure of **2** can be represented by the schematic diagram shown in Fig. 2 which is a scalene triangle of copper(II) centres. The Cu · · · Cu distances across the mesitylene spacer, *vis-à-vis* Cu(1,2) · · · Cu(3), are greater than 9 Å and, thus, these can be regarded as magnetically non-interactive. There are broadly two ways in which to approach the quantitative interpretation of the $\mu/T$ data shown in Fig. 3. First, by analogy to the structurally related trinuclear Schiff base $[Cu_3L(OH)]^{3+}$ complex reported by Fenton and co-workers[15] (Cu · · · Cu separations of 3.62, 4.95 and 5.89 Å and Cu–OH–Cu angle 138.2°) which has rather similar magnetic behaviour to **2** but with weaker coupling, it is possible to regard the latter as a dimer plus an independent monomer. The Cu(1)($\mu$-$HPO_4$)($\mu$-OH)Cu(2) moiety is expected to be the antiferromagnetically coupled binuclear unit whilst the Cu(1)-($\mu$-$HPO_4$)Cu(3) and Cu(2)($\mu$-$HPO_4$)Cu(3) units would be expected to be very weakly coupled, if at all. Secondly, the complex can be regarded as a non-symmetrical trinuclear $(Cu^{II})_3$ compound and various approximations can be made regarding its symmetry and relative values of $J$.

Starting with a dimer plus monomer approach, the susceptibility data were fitted by equation (1), where the parameters

$$\chi_m = (2N\beta^2 g_1^2/kT)[3 + \exp(-2J_{12}/kT)]^{-1} + N\beta^2 g_2^2/4kT) + N_\alpha \quad (1)$$

have their usual meanings and the $g$ values of the monomer and dimer were assumed to be different and $N_\alpha$ was set at $180 \times 10^{-6}$ $cm^3$ $mol^{-1}$ for the trinuclear moiety. The low-temperature plateau region fitted well, as anticipated, with $g_2 = 2.12$. It can be seen in Fig. 3(*a*) that the magnetic moment data in the region 60 to 300 K were also fitted reasonably well but the best-fit values of $g_1 = 2.10$ and $J_{12} = -161$ $cm^{-1}$ gave a crossing between observed and calculated data. Thus the curvature in the $\mu/T$ plot, which is sensitively influenced by $J_{12}$, was not replicated by equation (1). This contrasts with the excellent fit observed by Fenton and co-workers[15] for their Schiff-base system, although their use of a high $N_\alpha$ value set at $440 \times 10^{-6}$ $cm^3$ $mol^{-1}$ would influence the $J_{12}$ and $g_1$ values. As noted above, there were no bridging groups between the dimer and the monomer moieties present in that system.

The magnetic properties of intramolecularly coupled trinuclear $(Cu^{II})_3$ compounds have been summarised by Kahn[27] in his recent book. Kahn considered various symmetries such as equilateral, isosceles and scalene triangles of copper(II) ions and, in addition, linear and bent trinuclear. Spin-frustration effects in trimeric units were also discussed. A brief description of the situation for complex **2** is now given and the data are compared to the above-mentioned monomer + dimer approach in order to determine the most appropriate magnetic model for this interesting compound. In trinuclear models, the

Cu(1 or 2)(μ-$HPO_4$)Cu(3′) pathways containing three-atom bridging phosphates were initially anticipated to give weak coupling whilst the μ-hydroxo Cu(1)···Cu(2) pathway was assumed to give stronger antiferromagnetic coupling. Geometrically, the non-symmetrical (scalene) triangle of Cu(1), Cu(2) and Cu(3) should give three $J$ values and three energy levels consisting of a spin quartet and two spin doublets, the latter being mixed.[28] Under a $-2J_{12}S_1\cdot S_2 - 2J_{13}S_1\cdot S_3 - 2J_{23}S_2\cdot S_3$ Hamiltonian, the energies of these states are as given in equations (2) and (3).[27] The relative energies of the three

$$E(\tfrac{3}{2}) = -(2J_{12} + 2J_{13} + 2J_{23})/4 \quad (2)$$

$$E(\tfrac{1}{2},\pm) = \tfrac{1}{4}(2J_{12} + 2J_{13} + 2J_{23}) \pm \{[(2J_{12} - 2J_{13})^2 + (2J_{13} - 2J_{23})^2 + (2J_{23} - 2J_{12})^2]/8\}^{\frac{1}{2}} \quad (3)$$

states depend only on two energy gaps, $\Delta_1$ and $\Delta_2$ [equations (4)

$$\Delta_1 = E(\tfrac{1}{2},-) - E(\tfrac{1}{2},+) \quad (4)$$

and (5)], such that it is not possible to determine values of

$$\Delta_2 = E(\tfrac{3}{2}) - E(\tfrac{1}{2}+) \quad (5)$$

$J_{12}$, $J_{13}$ and $J_{23}$ unequivocally. These $J$ values consequently are highly correlated. If it is assumed that all molecular $g$ factors are equal,[29] then the susceptibility expression becomes (6). Fit-

$$\chi_m = \{(N\beta^2g^2/kT)[0.5 + 0.5\exp(-\Delta_1/kT) + 5\exp(-\Delta_2/kT)]/[2 + 2\exp(-\Delta_1/kT) + 4\exp(-\Delta_2/kT)]\} + N_\alpha \quad (6)$$

ting of the susceptibility data for complex **2** by equation (6) gave a very good fit for the parameter values $g = 2.10$, $N_\alpha = 180 \times 10^{-6}$ cm$^3$ mol$^{-1}$, $\Delta_1 = 92$ cm$^{-1}$, $\Delta_2 = 274$ cm$^{-1}$. The plot of calculated and observed moments is given in Fig. 3(*b*). Kahn and Gatteschi and co-workers[27,29] have pointed out that some simplifying assumptions need to be made in order to estimate individual $J$ values from $\Delta_1$ and $\Delta_2$ separations. In the case of a non-symmetrical, ferromagnetically coupled $[Cu_2V^{IV}O]^{2+}$ Schiff-base compound, Gatteschi and co-workers[29] estimated ranges of $J$ values by fixing one $J$ value at a structurally reasonable value (*e.g.* a very low value) and determining the other two. In the present case, we note that the $\Delta_1$ and $\Delta_2$ values are similar in size to those obtained using the symmetrical ABA trinuclear model (isosceles triangle) described below. Thus, the most reasonable assumption is to make $J_{13} = J_{23}$ since the Cu(1)···Cu(3) and Cu(2)···Cu(3) bridges are similar (Fig. 2). The values of $J_{12}$ and $J_{13}$ (=$J$) estimated from the best-fit values of $\Delta_1$ and $\Delta_2$, *vis-à-vis* $J = -90$ cm$^{-1}$ and $J_{12} = -45$ cm$^{-1}$, are, consequently, similar to those given below except for a small difference in $J_{12}$. The latter difference is not surprising in view of the insensitivity of the shape of the $\mu/T$ curve to $J_{12}$.

One of the most common geometries in trinuclear copper(II) systems is the isosceles triangle which employs the $-2J(S_1\cdot S_3 + S_2\cdot S_3) - 2J_{12}S_1\cdot S_2$ Hamiltonian, where $J_{12}$ refers to Cu(1)···Cu(2) coupling (Fig. 2) and $J$ to the Cu(1)···Cu(3) ~ Cu(2)···Cu(3) coupling.[11*h*,16,27–31] The energies $E(S,S^*)$ of the spin-quartet and two spin-doublet states are given in equations (7) to (9) where $S = (S_1 + S_2 + S_3)$ and $S^* = (S_1 + S_2)$. The

$$E(\tfrac{1}{2},1) = 2J - \tfrac{1}{2}J_{12} \quad (7)$$

$$E(\tfrac{1}{2},0) = 3J_{12}/2 \quad (8)$$

$$E(\tfrac{3}{2},1) = -J - \tfrac{1}{2}J_{12} \quad (9)$$

effect of $J_{12}$, for $J$ negative, is to influence the position of the $(\frac{1}{2},0)$ doublet state. At a fixed temperature it sensitively influences the size of $\mu_{eff}$[30] but has a smaller effect on the variation of $\mu_{eff}$ with $T$. The susceptibility expression for this situation is (10). The present magnetic moment data could be fitted

$$\chi_m = \{(N\beta^2g^2/4kT)[(\exp(-2J/kT) + \exp(-2J_{12}/kT) + 10\exp(J/kT)]/[\exp(-2J/kT) + \exp(-2J_{12}/kT) + 2\exp(J/kT)]\} + N_\alpha \quad (10)$$

extremely well by equation (10) using the parameters $g = 2.10$, $J = -90.3$ cm$^{-1}$, $J_{12} = -53.4$ cm$^{-1}$ and $N_\alpha = 180 \times 10^{-6}$ cm$^3$ mol$^{-1}$. The agreement between observed and calculated data is the same as that shown in Fig. 3(*b*). This fit yields the energies $E(\frac{3}{2},1) = 271$, $E(\frac{1}{2},0) = 74$ and $E(\frac{1}{2},1) = 0$ cm$^{-1}$. However, equally good fits were obtained for $J = -77$ to $-90$ cm$^{-1}$ and $J_{12} = -78$ to $-82$ cm$^{-1}$. Thus, we have a rare case in which $J$ and $J_{12}$ are correlated and rather insensitive within these ranges, the determining factor for best fit being the energy of the $E(\frac{3}{2},1)$ level. Slightly worse fits were obtained for $J$ held at $-90$ cm$^{-1}$ and $J_{12}$ varying between $-55$ and $-80$ cm$^{-1}$. If $J$ is set to zero, a good least-squares fit is obtained for $J_{12} = -150$ cm$^{-1}$, but the calculated and observed $\mu/T$ curves cross at *ca.* 180 K. If we assume that the best-fit $J$ and $J_{12}$ ranges are correct and are as defined in Fig. 2(*b*) then we have the unexpected situation that the two three-atom phosphato bridge provides similar antiferromagnetic coupling to the shorter μ-hydroxo, μ-phosphato bridge. There are few quantitative studies of three-atom phosphato-bridged copper(II) compounds available for comparison. The work of Ainscough *et al.*[32] would suggest that such bridges should provide very small $J$ values. A recent study by Ranford and co-workers[33] of an associated dinuclear compound of the type $[\{Cu_2(HL)(H_2PO_4)_2\}_2][NO_3]_2\cdot 2H_2O$, where $H_2L$ = 2,2′-bis[1-(2-pyridyl)methylidene]thiocarbonylbis(hydrazine), shows a rather similar three-atom bridging $H_2PO_4^-$ to that of $HPO_4^{2-}$ in **2** but disposed in axial–equatorial positions with respect to adjacent copper(II) centres. The $J$ value attributed to the Cu(μ-$H_2PO_4$)Cu moiety was found to be $-16$ cm$^{-1}$. It is possible that a $J$ value of larger magnitude is present for **2**. In the case of the double bridge in **2**, between Cu(1) and Cu(2), the equatorial planes O(3)N(3)N(2)O(1) around Cu(1) and O(2)N(6)N(5)O(1) around Cu(2) are hinged at O(1) with a dihedral angle (δ) between them of 31.8° and have the O(2)–P(1)–O(3) bridging phosphate atoms disposed in a similar fashion to that found recently in related μ-$RCO_2$, μ-OH bridged complexes. Indeed Chakravarty and co-workers[34] have proposed that a linear relationship exists between $J_{12}$ and the Cu···Cu distance, and $J_{12}$ and δ. Counter-complementary effects between the overlap of copper d orbitals and the $OH^-$ and $RCO_2^-$ orbitals were invoked to explain the size of $J_{12}$. The present $J_{12}$ value of $-53$ or *ca.* $-80$ cm$^{-1}$ gives reasonable agreement with their calculations. The effect on $J_{12}$ when changing from carboxylate to phosphate is not yet known. Thus, while the expectation at the outset was for $J$ to be much less than $J_{12}$ in **2**, when using equation (10), the comparisons just given to the very few available related systems suggest that best-fit values of $J$ and $J_{12}$ may well be reasonable.

In assessing the various models used to analyse the magnetic data for compound **2**, we believe that the isosceles triangle approximation with $J$ and $J_{12}$ both non-zero and negative is the best. Simplification of the asymmetric triangle model leads to the same values of $J$ and $J_{12}$.

We turn now to the X-band ESR spectra of complex **2** to see if they shed further light on the most appropriate magnetic model. The spectrum of a neat powdered sample at 77 K is shown in Fig. 4(*a*). In comparison to the broad spectra usually obtained for neat powders, there are six equally spaced components of a probable seven-line copper hyperfine multiplet evident between 2500 and 3100 G with a separation of 77 G as well as a strong *x*, *y* resonance at *ca.* 3200 G. The line shape is most likely due to weak copper(II)-pair interactions (analysis of the spectrum gave $g_\perp = 2.060$, $g_\parallel = 2.275$;

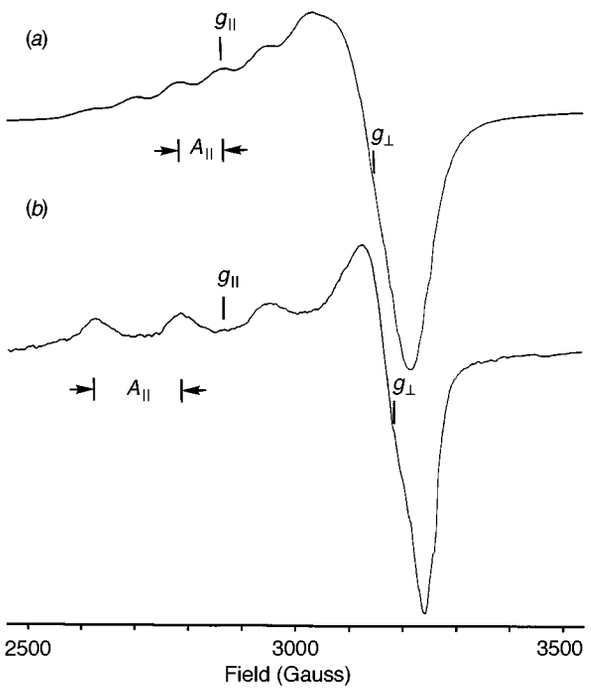


**Fig. 4** X-Band ESR spectrum of (*a*) a neat powder of complex **2** and (*b*) a frozen dmf solution of **2**, recorded at 77 K

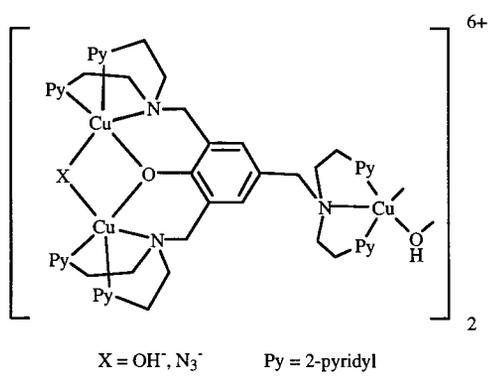


**Fig. 5** Schematic diagram of the hexanuclear framework of the complex reported by Karlin *et al.*[12]

$A_{\|} = 85 \times 10^{-4}$ cm$^{-1}$), although it may also be due to the superimposition of $S = \frac{1}{2}$ signals from both the ($\frac{1}{2}$,1) and ($\frac{1}{2}$,0) levels, both of which are thermally accessible at 77 K. The spectrum remains well resolved at temperatures below 77 K but it is broadened by spin–lattice relaxation effects at higher temperatures. The spectra recorded in frozen dilute dmf [shown in Fig. 4(*b*)] and water–glycol (1:1) solutions are identical ($g_{\perp} = 2.05$, $g_{\|} = 2.28$; $A_{\|} = 171 \times 10^{-4}$ cm$^{-1}$) and are similar to the axial line shape observed for the uncoupled complex **1**. These spectra are characteristic of a monomeric tetragonal copper(II) complex and in the case of **2** indicate that dissolution results in formation of an uncoupled copper(II) centre, although it should be recognised that traces of monomer impurity could give rise to the same behaviour. Since the trinuclear sites in **2** are part of a polymeric network in the crystalline state, it is reasonable to suggest that the high solubility of the complex is due to dissociation and protonation of some of the bridging groups on dissolution. Total dissociation of the bridging groups would generate a solution of **1**, with different counter ions, and an ESR spectrum very similar to **1** would be expected. However, it is difficult to rationalise the dissociation of the hydroxo bridge since under the conditions used the likely source of protons, $HPO_4^{2-}$, is a very weak acid. The most likely explanation is that the polymer dissociates in solution to form $[Cu_2(\mu\text{-OH})(\mu\text{-HPO}_4)LCu(OH_2)]^{3+}$ trinuclear units. In this form, the μ-OH, μ-$HPO_4$ linked Cu(1)···Cu(2) pair is ESR silent due to the persistence of moderate-strength coupling and consequently only the monomeric copper(II) centre is observed. The $^{31}$P NMR spectrum of the complex in dmf is consistent with this proposal, showing a multiplet for the $PF_6^-$ counter ion and no signal due to bridging phosphate. However, a signal attributable to free phosphate does appear when acid is added to dissociate the complex. The persistence of the trinuclear unit in solution is further demonstrated by the electrospray mass spectrum of **2** run in aqueous solution. This confirmed the presence of ionic species with composition and copper isotope distribution patterns for $[Cu_3L(\mu\text{-OH})(\mu\text{-HPO}_4)(PF_6)_2]^+$ ($m/z = 1095$), $[Cu_3L(\mu\text{-OH})(\mu\text{-PO}_4)(PF_6)]^+$ ($m/z = 950$) and $[Cu_3L(\mu\text{-OH})(\mu\text{-PO}_4)]^{2+}$ ($m/z = 402.6$), where the quoted $m/z$ values represent the most intense peak in the isotope distribution pattern. The behaviour of **2** corresponds to that of the hexanuclear copper(II) complex shown in Fig. 5 which in coordinating solvents like dmf and MeOH dissociates to a trinuclear complex with two endogenously linked, ESR-silent copper(II) centres (type 3) and a third copper(II) centre which behaves like a type 2 copper site. The solution ESR parameters of **2** and this complex are similar to those of Lc and AO, where the parameter ranges for the type 2 centre are $g_{\|} = 2.23$–$2.26$, $g_{\perp} = 2.04$–$2.06$ and $A_{\|} = (170$–$200) \times 10^{-4}$ cm$^{-1}$.[1b,10] We note, however, that this sensitive resonance technique is notorious for yielding monomer signals for what are otherwise regarded as strongly coupled di- or tri-nuclear species which intrinsically should not show such signals.[34]

Returning to the solid state, the magnetic data on a powdered sample (see above) show that the compound is essentially in an $S = \frac{1}{2}$ state at 77 K. Often such ABA trinuclear systems of linear or bent geometry, and with very large and negative $J_{12}$ values, display two-line axial or three-line rhombic $S = \frac{1}{2}$ ESR spectra when measured at 10 K and no hyperfine splitting has been observed in these cases.[11h,35] The spectral shapes are therefore different to those in Fig. 4(*a*) but the $g_z$ and $g_{x,y}$ values are rather similar in size to their counterparts in **2**. The powder spectrum of Fenton and co-workers[15] trinuclear complex at 4 K was broad ($g \approx 2.10$) and uninformative. It is therefore difficult to draw any firm conclusions from the powder ESR spectrum in relation to the various models used to interpret the magnetism. Variable-temperature data confirm that the observed spectrum is intrinsic to the trinuclear complex but line broadening at $T > 77$ K makes it difficult to know if ($\frac{1}{2}$,0) and ($\frac{3}{2}$,1) levels became populated. Solomon and co-workers[28] have emphasised this point in their discussion of the asymmetric trinuclear model [equations (2) and (3)] when applied to the resting and ligand-bound forms of Lc.

Finally, we comment briefly on the possible relevance of the present model study to the physical properties of solutions of the multicopper enzymes, Lc and AO. Solomon *et al.*[10] have recently summarised their detailed spectroscopic (UV/VIS, MCD, ESR and extended X-ray absorption fine structure, EXAFS) and SQUID susceptibility data for various forms of these enzymes including those which are type 2 copper depleted or in which the type 1 copper is replaced by mercury (type 1 Hg). It is important to note that it has been often postulated that the enzymes adopt different trinuclear structures in solution, *e.g.* azide- or peroxo-bound laccase, compared to the crystal structures of these forms, particularly in regard to Cu···Cu separations and bridging geometries. The data for complex **2** are not the same as those observed for oxidised AO or Lc which is not surprising in view of the structure, for instance, of AO which contains a three-co-ordinate type 2 copper not bridged to the type 3 copper, these being placed at 3.66 and 3.78 Å away. The latter are each four-co-ordinate with a proposed pseudo-trigonal bipyramidal geometry, the apical $z$ direction of each meeting the OH bridging oxygen atom. The strong antiferromagnetic coupling across this Cu–OH–Cu bridge ($-2J > 400$ cm$^{-1}$) most likely results from overlap of the Cu ($d_{z^2}$) and O (p)

orbitals.[10] In **2** the bridging orbitals to the OH group are Cu ($d_{x^2-y^2}$) and a second bridging (phosphate) group completes the five-co-ordinate geometry about each Cu. The resulting $J_{12}$ value is less than that of AO. Magnetic and ESR studies of the present type also provide broad and useful comparisons with other forms of the enzyme. In the case of the oxygen intermediate of native Lc, spectroscopic studies indicate that the trinuclear site contains an unsymmetrical trinuclear cluster with hydroxide bridges between the type 2 copper and only one of the type 3 copper centres as well as a hydroxide bridge between the type 3 copper centres[10,36] (notably, although this model is 'spectroscopically effective' it differs from the crystal structure of the peroxide adduct of AO[10]). The native Lc oxygen intermediate has an $S = \frac{1}{2}$ ground state with an unusual $g = 1.94$ ESR signal which is clearly different to the spectrum of **2** and, to our knowledge, unprecedented in the trinuclear copper model studies. Interestingly, an oxygen intermediate of type 1 Hg Lc gave susceptibility data indicative of a smaller $J$ value, *vis-à-vis* $-2J > 200$ cm$^{-1}$, but this could not be assigned unambigously to the type 3 Cu–OH–Cu bridge or the proposed Cu (type 3)–O(OH)–Cu (type 2) μ-1,1-$HO_2^-$ bridge.‡ Our ongoing studies of the reaction of **1** and **2** with hydrogen peroxide and of the copper(I) complex of L, *vis-à-vis* $[Cu_3L(CH_3CN)_3]^{3+}$, with dioxygen may prove instructive in this regard.

## Acknowledgements

Financial support in the form of Australian Research Council Grants (to L. S. and K. S. M.) and an Australian Postgraduate Award (to B. G.) is acknowledged. We thank Ms. S. Duck for the measurement of electrospray mass spectra and Mr. K. J. Berry for assistance with the fitting of the magnetic susceptibility data.

‡ *Note added at proof*. A recent SQUID and E study[37] of laccase and ascorbate oxidase showed $\mu_{eff}/T$ plots rather similar to those shown in Fig. 3 but with the increase in $\mu_{eff}$ occurring above 200 K for AO and azide-bound Lc. The smaller $J$ values ($\approx -170$ cm$^{-1}$) were ascribed to weaker type 3 coupling or to switching of the OH bridge from type 3 to type 3–type 2 copper centres.

## References

1 For recent reviews, see (*a*) K. D. Karlin, Z. Tyeklár and A. D. Zuberbühler, in *Bioinorganic Catalysis*, ed. J. Reedjik, Marcel Dekker, New York, 1993, p. 261; (*b*) A. Messerschmidt, *Adv. Inorg. Chem*., 1993, **40**, 121; (*c*) V. McKee, *Adv. Inorg. Chem*., 1993, **40**, 323; (*d*) N. Kitajima and Y. Moro-oka, *Chem. Rev*., 1994, **94**, 737; (*e*) E. I. Solomon, F. Tuczek, D. E. Root and C. A. Brown, *Chem. Rev*., 1994, **94**, 827; (*f*) K. D. Karlin and Z. Tyeklár, *Adv. Inorg. Biochem*., 1994, **9**, 123; (*g*) W. Kaim and B. Schwederski, *Bioinorganic Chemistry: Inorganic Elements in the Chemistry of Life*, Wiley, Chichester, 1995; (*h*) W. Kaim and J. Rall, *Angew. Chem*., *Int. Ed. Engl*., 1996, **35**, 43 and refs. therein.

2 N. Kitajima, K. Fujisawa and Y. Moro-oka, *J. Am. Chem. Soc*., 1989, **111**, 8975; N. Kitajima, T. Koda, Y. Iwata and Y. Moro-oka, *J. Am. Chem. Soc*., 1990, **112**, 8833; N. Kitajima, T. Koda, S. Hashimoto, T. Kitagawa and Y. Moro-oka, *J. Am. Chem. Soc*., 1991, **113**, 5664; N. Kitajima and Y. Moro-oka, *J. Chem. Soc*., *Dalton Trans*., 1993, 2665; K. Fujisawa, M. Tanaka, Y. Moro-oka and N. Kitamima, *J. Am. Chem. Soc*., 1994, **116**, 12079.

3 P. P. Paul, Z. Tyeklár, R. R. Jacobson and K. D. Karlin, *J. Am. Chem. Soc*., 1991, **113**, 5322; D.-H. Lee, N. N. Murthy and K. D. Karlin, *Inorg. Chem.*, 1996, **35**, 804; K. D. Karlin, D.-H. Lee, S. Kaderli and A. D. Zuberbühler, *Chem. Commun*., 1997, 475; R. J. M. Klein Gebbink, C. F. Martens, M. C. Feiters, K. D. Karlin and R. J. M. Nolte, *Chem. Commun*., 1997, 389.

4 C. J. Cramer, B. A. Smith and W. B. Tolman, *J. Am. Chem. Soc*., 1996, **118**, 11283; S. Mahapatra, J. A. Halfen, E. C. Wilkinson, G. Pan, X. Wang, V. C. Young, jun., C. J. Cramer, L. Que, jun. and W. B. Tolman, *J. Am. Chem. Soc*., 1996, **118**, 11555; S. Mahapatra, V. C. Young jun., S. Kaderli, A. D. Zuberbühler and W. B. Tolman, *Angew. Chem*., *Int. Ed. Engl*., 1997, **36**, 130.

5 L. Casella, E. Monzani, M. Gullotti, D. Cavagnino, G. Cerina, L. Santagostini and R. Ugo, *Inorg. Chem*., 1996, **35**,7516.

6 D. A. Rockcliffe, A. E. Martell and J. H. Reibenspies, *J. Chem. Soc*., *Dalton Trans.*, 1996, 167.

7 L. J. Farrugia, P. A. Lovatt and R. D. Peacock, *J. Chem. Soc*., *Dalton Trans.*, 1997, 911.

8 (*a*) A. Messerschmidt, A. Rossi, R. Ladenstein, R. Huber, M. Bolognesi, G. Gatti, A. Marchesini, R. Petruzzelli and A. Finazzi-Agro, *J. Mol. Biol*., 1989, **206**, 513; (*b*) A. Messerschmidt, R. Ladenstein, R. Huber, M. Bolognesi, L. Avigliano, R. Petruzzelli, A. Rossi and A. Finazzi-Agro, *J. Mol. Biol*., 1992, **224**, 179.

9 A. Messerschmidt, H. Luecke and R. Huber, *J. Mol. Biol*., 1993, **230**, 997.

10 E. I. Solomon, U. M. Sundaram and T. E. Machonkin, *Chem. Rev*., 1996, **96**, 2563.

11 See, for example, (*a*) R. Beckett and B. F. Hoskins, *J. Chem. Soc*., *Dalton Trans*., 1972, 291; (*b*) R. J. Butcher, C. J. O'Connor and E. Sinn, *Inorg. Chem*., 1981, **20**, 537; (*c*) F. B. Huisbergen, R. W. M. ten Hoedt, G. C. Verschoor, J. Reedjik and A. L. Spek, *J. Chem. Soc*., *Dalton Trans.*, 1983, 539; (*d*) J. P. Costes, F. Dahan and J. P. Laurent, *Inorg. Chem*., 1986, **25**, 413; N. A. Bailey, D. E. Fenton, R. Moody, P. J. Scrimshire, E. Belortzky, P. H. Fries and J. M. Latour, *J. Chem. Soc*., *Dalton Trans*., 1988, 2817; (*e*) K. D Karlin, Q.-F. Gan, A. Farooq, S. Liu and J. Zubieta, *Inorg. Chim. Acta*, 1989, **165**, 37; (*f*) M. Angaroni, G. A. Ardizzoia, T. Beringhelli, G. L. Monica, D. Gatteschi, N. Masciochhi and M. Moret, *J. Chem. Soc*., *Dalton Trans*., 1990, 3305; (*g*) Y. Angus, R. Louis, B. Metz, C. Bouden, J. P. Gisselbrecht and M. Gross, *Inorg. Chem*., 1991, **30**, 3155; (*h*) P. Chaudhuri, M. Winter, B. P. C. Della Vedova, E. Bill, A. Trautwein, S. Gehring, P. Fleisschhauer, B. Nuber and J. Weiss, *Inorg. Chem.*, 1991, **30**, 2148; (*i*) S. Meenkumari and A. R. Chakravarty, *J. Chem. Soc*., *Dalton Trans*., 1992, 2749; (*j*) D. Christodoulou, C. George and L. K. Keefer, *J. Chem. Soc*., *Chem. Commun*., 1993, 937; (*k*) P. J. van Konings-bruggen, J. W. van Hal, R. A. G. de Graaf and J. G. Reedijk, *J. Chem. Soc*., *Dalton Trans*., 1993, 2163.

12 K. D. Karlin, Q.-F. Gan, A. Farooq, S. Liu and J. Zubieta, *Inorg. Chem*., 1990, **29**, 2549.

13 P. Chaudhuri, I. Karpenstein, M. Winter, C. Butzlaff, E. Bill, A. X. Trautwein, U. Flörke and H.-J. Haupt, *J. Chem. Soc*., *Chem. Commun*., 1992, 321.

14 D. E. Fenton, in *Perspectives in Coordination Chemistry*, eds. A. F. Williams, C. Floriani and A. E. Merbach, VCH, Basel, 1992, p. 203; D. E. Fenton and H. Okawa, *J. Chem. Soc*. *Dalton Trans*., 1993, 1349.

15 H. Adams, N. A. Bailey, M. J. S. Dwyer, D. E. Fenton, P. C. Hellier, P. D. Hempstead and J. M. Latour, *J. Chem. Soc*., *Dalton Trans*., 1993, 1207.

16 S. Meenakumari, S. K. Tiwary and A. R. Chakravarty, *Inorg. Chem*., 1994, **33**, 2085.

17 A. P. Cole, D. E. Root, P. Mukherjee, E. I. Solomon and T. D. P. Stack, *Science*, 1996, **273**, 1848.

18 E. Hough, L. K. Hansen, B. Birknes, K. Jynge, S. Hansen, A. Hordvik, C. Little, E. Dodson and Z. Derewanda, *Nature* (*London*), 1989, **338**, 357; A. Volbeda, A. Lahm, F. Sakiyama and D. Suck, *EMBO J*., 1991, **10**, 1607; S. Hansen, L. K. Hansen and E. Hough, *J. Mol. Biol.*, 1992, **225**, 543.

19 X. Zhang, W.-Y. Hsieh, T. N. Margulis and L. J. Zompa, *Inorg. Chem*., 1995, **34**, 2883.

20 F. Vögtle, M. Zuber and R. G. Lichtenthaler, *Chem. Ber*., 1973, **106**, 717.

21 N. Walker and D. Stuart, *Acta Crystallogr*., *Sect. A*, 1983, **39**, 158.

22 P. T. Buerskens, G. Admiraal, G. Buerskens, W. P. Bosman, S. Garcia-Granda, J. M. M. Smits and C. Smykalla, The DIRDIF program system, Technical Report of the Crystallography Laboratory, University of Nijmegen, 1992.

23 TEXSAN, Crystal Structure Analysis Package, Molecular Structure Corporation, Houston, TX, 1985.

24 C. K. Johnson, ORTEP II, Report ORNL-5136, Oak Ridge National Laboratory, Oak Ridge, TN, 1976.

25 (*a*) A. E. Gebala and M. M. Jones, *J. Inorg. Nucl. Chem*., 1969, **31**, 771; (*b*) I. G. Ryss and V. B. Tul'chinskii, *Zh. Neorg. Khim*., 1967, **9**, 836; (*c*) T. Koike, S. Kajitani, I. Nakamura, E. Kimura and M. Shiro, *J. Am. Chem. Soc*., 1995, **117**, 1210.

26 W. F. Schwindinger, T. G. Fawcett, R. A. Lalancette, J. A. Potenza and H. J. Schugar, *Inorg. Chem.*, 1980, **19**, 1379; R. D. Bereman, M. W. Churchill, P. M. Schaber and M. E. Winkler, *Inorg. Chem*., 1979, **18**, 3122.

27 O. Kahn, *Molecular Magnetism*, VCH, New York, 1993, ch. 10, p. 211.

28 J. L. Cole, P. A. Clark and E. I. Solomon, *J. Am. Chem. Soc*., 1990, **112**, 9534.
29 A. Bencini, C. Benelli, A. Dei and D. Gatteschi, *Inorg. Chem*., 1985, **24**, 695.
30 S. J. Gruber, C. M. Harris and E. Sinn, *J. Chem. Phys*., 1968, **49**, 2183.
31 W. Haase and S. Gehring, *J. Chem. Soc*., *Dalton Trans.*, 1985, 2609.
32 E. W. Ainscough, A. M. Brodie, J. D. Ranford and J. M. Waters, *J. Chem. Soc*., *Dalton Trans*., 1997, 1251.
33 B. Moubaraki, K. S. Murray, J. D. Ranford, X. Wang and Y. Xu, unpublished work.
34 S. Meenakumari, S. K. Tiwary and A. R. Chakravarty, *J. Chem. Soc.*, *Dalton Trans.*, 1993, 2175.
35 R. Veit, J.-J. Girerd, O. Kahn, F. Robert and Y. Jeannin, *Inorg. Chem*., 1986, **25**, 4175.
36 E. I. Solomon, M. J. Baldwin and M. D. Lowery, *Chem. Rev*., 1992, **92**, 521.
37 T. Sakurai, H. Huang, H. Monjushiro and S. Takeda, *J. Bioinorg. Chem.*, 1997, **67**, 57.

*Received* 23*rd June* 1997; *Paper* 7/04397J